Far-Red Excitation Induced Electron Transfer in Bis Donor-AzaBODIPY Push-Pull Systems; Role of Nitrogenous Donors in Promoting Charge Separation

Ajyal Z. Alsaleh,[a] Dilip Pinjari,[b] Rajneesh Misra,[b]* Francis D'Souza,[a]*

---

[a] A. Z. Alsaleh and Prof. Dr. F. D'Souza

Department of Chemistry, University of North Texas, Denton, TX 76203-5017, USA

E-mail: Francis.Dsouza@unt.edu

https://chemistry.unt.edu/people-node/francis-dsouza

[b] D. Pinjari and Prof. Dr. R. Misra

Department of Chemistry, Indian Institute of Technology, Indore 453552, India.

E-mail: rajneeshmisra@iiti.ac.in

https://chemistry.iiti.ac.in/people/faculty/prof-rajneesh-misra/

Supporting Information is available for this article on the WWW under https://doi...

^{1}H, ^{13}C, ^{11}B, and ^{19}F NMR and HRMS of synthesized compounds; additional spectral data.

Abstract

A far-red absorbing sensitizer, BF_2-chelated azadipyrromethane (azaBODIPY) has been employed as an electron acceptor to synthesize a series of push-pull systems linked with different nitrogenous electron donors, viz., *N,N*-dimethylaniline (NND), triphenylamine (TPA), and phenothiazine (PTZ) *via* an acetylene linker. The structural integrity of the newly synthesized push-pull systems was established by spectroscopic, electrochemical, spectroelectrochemical, and DFT computational methods. Cyclic and differential pulse voltammetry studies revealed different redox states and helped in the estimation of the energies of the charge-separated states. Further, spectroelectrochemical studies performed in a thin-layer optical cell revealed diagnostic peaks of azaBODIPY$^{\bullet-}$ in the visible and near-IR regions. Free-energy calculations revealed the charge separation from one of the covalently linked donors to the ^{1}azaBODIPY* to yield Donor$^{\bullet+}$-azaBODIPY$^{\bullet-}$ to be energetically favorable in a polar solvent, benzonitrile, and the frontier orbitals generated on the optimized structures helped in accessing such a conclusion. Consequently, the steady-state emission studies revealed quenching of the azaBODIPY fluorescence in all of the investigated push-pull systems in benzonitrile and to a lesser extent in mildly polar dichlorobenzene, and nonpolar toluene. The femtosecond pump-probe studies revealed the occurrence of excited charge transfer (CT) in nonpolar toluene while a complete charge separation (CS) for all three push-pull systems in polar benzonitrile. The CT/CS products populated the low-lying ^{3}azaBODIPY* prior to returning to the ground state. Global target (GloTarAn) analysis of the transient data revealed the lifetime of the final charge-separated states (CSS) to be 195 ps for NND-derived, 50 ps for TPA-derived, and 85 ps for PTZ-derived push-pull systems in benzonitrile.

Introduction

The study of multi-modular donor-acceptor constructs[1–8] has played a prominent role in a range of applications in energy harvesting, organic electronics, and photonics.[9–17] In this scenario, the use of a π-bridge to covalently connect the donor and acceptor entities is recognized as a means to enhance intramolecular charge transfer (ICT) in the excited state and finely adjust the optical and excited-state properties. Furthermore, when employed in polar solvents, these ICT states have the potential to transition into a fully separated state with complete charge transfer.[18–20] The persistence of charge separated state however depends on the low-lying triplet states of either the donor or acceptor. In such instances, the charge recombination (CR) could occur rapidly thus lowering their overall lifetime. In synthetic artificial photosynthetic systems, long-lived charge-separated states (CSS) are often achieved by optimal positioning of the donor and acceptor systems and following a multi-step sequential electron transfer mechanism.[21–26] In a few instances, heavy atom-bearing high-energy triplet sensitizers have also been used to build donor-acceptor constructs to achieve long-lived CSS.[27,28]

Among the electron donor or acceptor photosensitizers, BF_2-chelated azadipyrromethene (abbreviated azaBODIPY),[29] a structural analog of BF_2-chelated dipyrromethene (BODIPY®),[30,31] has recently gained much attention for its novel photochemical properties, applicable in energy harvesting, sensing and imaging applications.[29,30] Depending upon the peripheral substituents, azaBODIPYs absorb in the 300–850 nm region with very high molar absorptivity and desirable emission in the red to the near-IR region (660–900 nm) with quantum yields exceeding 40%.[31] One of the most interesting properties of azaBODIPYs is in their facile reduction making them rarely encountered electron acceptor far-red capturing photosensitizer molecules.[32] In addition, azaBODIPYs are now being explored for applications involving near-IR absorbing dyes for biological applications,[33] photocatalysts,[34] and triplet photosensitizers.[35]

In recent years, we have been involved in exploring novel features of azaBODIPY in photoinduced charge separation and stabilization, useful for light energy conversion and optoelectronic materials. To summarize our key findings, when azaBODIPY was connected to ferrocene, efficient photoinduced reductive electron transfer (PET) from ferrocene to ^{1}azaBODIPY* to yield Fc^+-azaBODIPY$^{\bullet-}$ was witnessed.[36] Alternatively, when ferrocene was replaced by fullerene, C_{60}, oxidative electron transfer leading to the formation of azaBODIPY$^{\bullet+}$-

$C_{60}^{\bullet-}$ was observed.[37] Excitation transfer was observed when either chlorophyll derivatives or BODIPY was covalently linked to azaBODIPY.[38] Interestingly, when two porphyrins were covalently linked to azaBODIPY, the resulting 'molecular clip' supramolecularly bound to C_{60} via metal-ligand coordination. In this molecular system, energy and electron transfer events were possible to regulate.[39] Furthermore, by a combination of zinc porphyrin, BODIPY, and azaBODIPY, a novel broad-band capturing and emitting supramolecular push-pull system capable of wide-band emission was recently reported.[40] Supramolecular donor-acceptor hybrids of zinc phthalocyanine (ZnPc)-azaBODIPY and zinc naphthalocyanine (ZnNc)-azaBODIPY, that is, near-infrared absorbing entities, were constructed and photoinduced electron transfer by near-IR excitation was witnessed,[41] wherein $ZnPc^{\bullet+}$- $azaBODIPY^{\bullet-}$ and $ZnNc^{\bullet+}$- $azaBODIPY^{\bullet-}$ were the reaction products. Directly connected azaBODIPY-donor systems exhibiting intramolecular charge transfer were also reported.[42] More recently, azaBODIPY was covalently linked to powerful electron acceptors, tetracyanobutadiene (TCBD) and extended-TCBD, and the occurrence of excited state charge transfer was successfully demonstrated.[43] These are in addition to studies reported by other groups.[44–55]

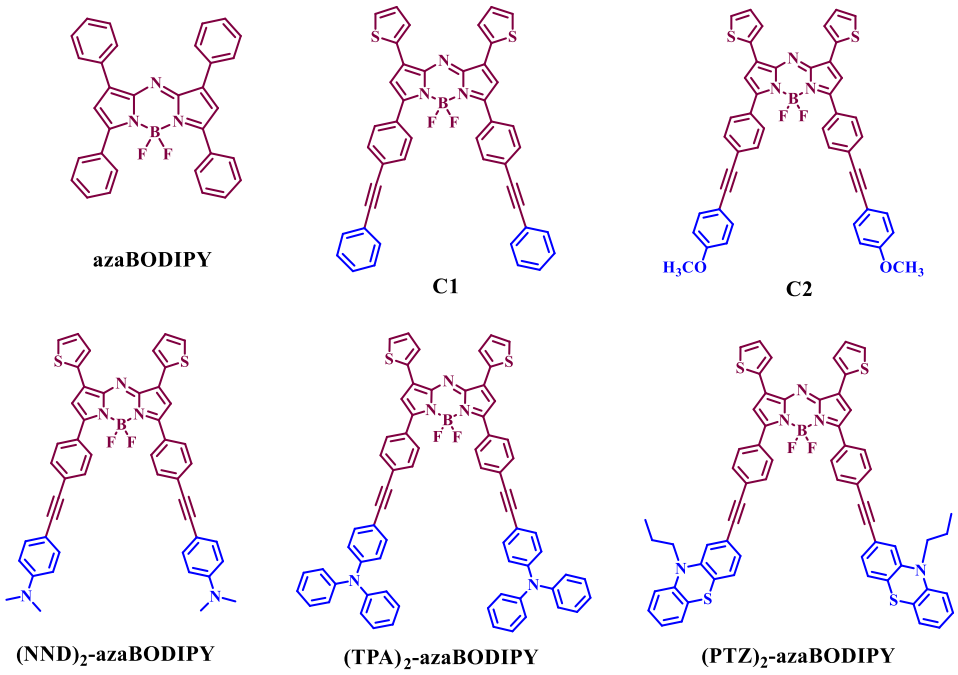

Figure 1. Structures and abbreviations of pristine azaBODIPY, control azaBODIPYs carrying ethynyl linkers, and nitrogenous amine donors carrying azaBODIPY push-pull systems studied in the present investigation.

In the present study, we report a new series of bisdonor-acceptor push-pull systems featuring nitrogenous electron donors, viz., *N,N*-dimethylaniline (NND), triphenylamine (TPA), and phenothiazine (PTZ) with the help of acetylene linkers (see Figure 1 for structures along with those of the control compounds). Here, the azaBODIPY core is different from the traditionally used azaBODIPY in which two β-pyrrole-phenyl rings have been replaced with thiophene units and the α-phenyl groups have acetenyl-phenyl entities. The immediate consequence of this small structural change is in extending the absorption envelope by 40 nm to the red making them far-red absorbers. The significance of the nitrogenous donors in governing far-red excited state charge transfer/separation as a function of solvent polarity is presented. Our studies demonstrate that in nonpolar toluene, the push-pull systems undergo partial charge transfer while in polar, benzonitrile, they undergo full charge separation. The persistence of the charge-separated state (CSS) with respect to the nature of the donor, as revealed by transient pump-probe spectroscopic studies is presented.

Results and Discussion

Synthesis of different donor substituted aza-BODIPY derivatives namely **(NND)$_2$-azaBODIPY**, **(TPA)$_2$-azaBODIPY**, **(PTZ)$_2$-azaBODIPY** along with control azaBODIPYs (**C1**, **C2**) is shown in Scheme 1. Dibromo-aza-BODIPY **1** was reacted with various ethynyl substituted aryl derivatives (phenyl, anisole, *N,N*-dimethylamine, triphenylamine and phenothiazine) under Pd-catalyzed Sonogashira coupling reaction to obtain **C1**, **C2**, **(NND)$_2$-azaBODIPY**, **(TPA)$_2$-azaBODIPY**, **(PTZ)$_2$-azaBODIPY** with 85%, 80%, 75%, 82%, and 77% yield, respectively. This reaction was carried out in a THF/TEA mixture (v/v,1:1) with Pd-catalyst at 60 ^{o}C for 12 hrs under an argon atmosphere. The synthesis of triphenylamine based aza-BODIPY (**TPA**)$_2$**-azaBODIPY** was recently reported by us.[43] The precursor dibromo-aza-BODIPY **1** was synthesized using a reported procedure by reacting thiophene-2-carbaldehyde with 4-bromo-acetophenone.[56]

All the aryl substituted azaBODIPY derivatives (**C1**, **C2**, **(NND)$_2$-azaBODIPY**, **(TPA)$_2$-azaBODIPY**, **(PTZ)$_2$-azaBODIPY**) were purified by using neutral activated alumina. These conjugates are soluble in common organic solvents, such as chloroform, toluene, DCM, and were well characterized using ^{1}H NMR, ^{13}C NMR, and HRMS techniques (see the SI for spectral details, Figures S1–S22).

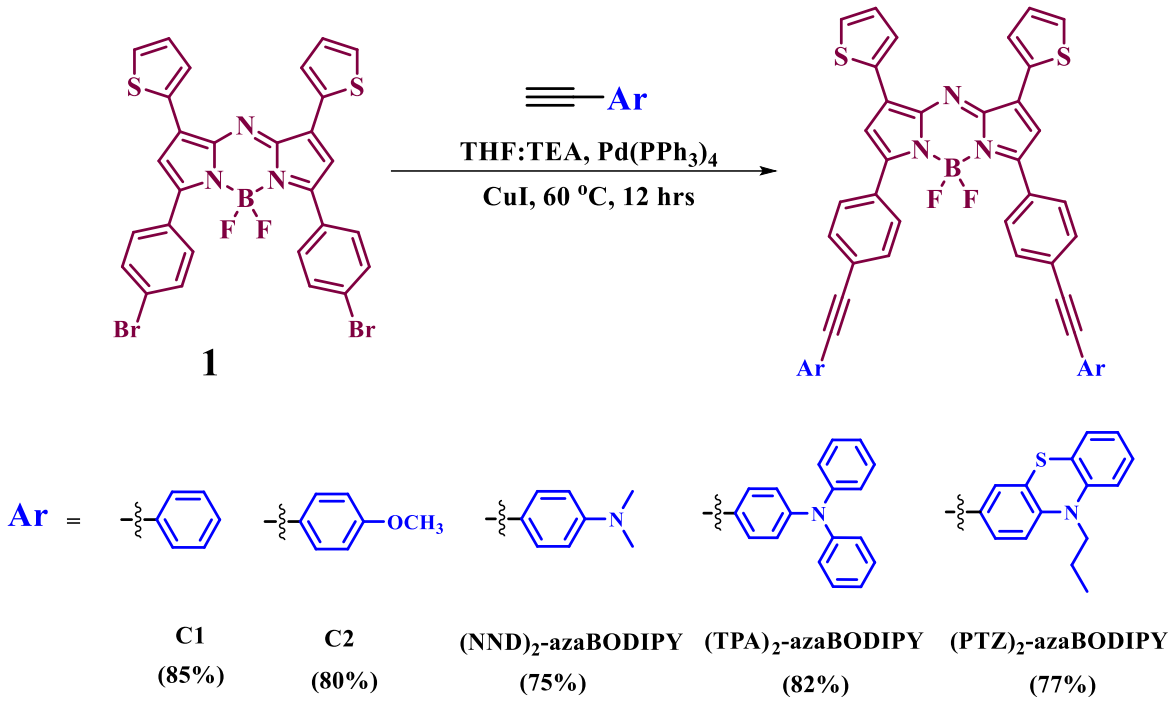

Scheme 1. Synthetic route for various aryl functionalized azaBODIPY donor-acceptor constucts.

Optical absorption and fluorescence studies

The absorption and fluorescence spectra of the investigated compounds in benzonitrile, DCB, and toluene are depicted in Figure 2 while the optical data are summarized in Table 1. In benzonitrile, the pristine **azaBODIPY** peak located at 671 nm was shifted to 724 and 731 nm in **C1** and **C2**, respectively. That is, a 43–49 nm red shift as a consequence of the peripheral substitution of thiophene and phenyl-acetenyl entities was witnessed. Appending electron donors further shifted the peak maxima to another 20–30 nm depending on the type of donor entities. These observations suggest electronic interactions between the azaBODIPY and donor entities via the acetenyl linkers. Such a trend was also observed in DCB and toluene. For example, in toluene, a 46–51 nm red-shift between **azaBODIPY** and **C1**/**C2** and a further 20–30 nm after appending the electron donor entities.

Table 1. Optical absorption and emission data for the investigated compounds in solvents of varying polarity.

Compound	Solvent	λ_{abs}, nm	λ_{em}, nm	$E_{0,0}$	Φ_f
azaBODIPY	PhCN	326, 511, 671	702	1.80	0.23[a]
C1		358, 551, 724	751	1.68	0.028
C2		320, 552, 732	762	1.66	0.016
(NND)$_2$-azaBODIPY		359, 609, 758	--	--	--
(TPA)$_2$-azaBODIPY		367, 590, 745	--	--	--
(PTZ)$_2$-azaBODIPY		365, 584, 744	--	--	--
azaBODIPY	DCB	315, 503, 670	700	1.80	0.23[a]
C1		356, 542,727	752	1.68	0.30
C2		350, 521, 737	763	1.65	0.025
(NND)2-azaBODIPY		359, 615, 761	828	1.56	0.010
(TPA)2-azaBODIPY		371, 594, 751	--	--	--
(PTZ)2-azaBODIPY		369, 570, 745	--	--	--
azaBODIPY	Toluene	300, 506, 663	686	1.83	0.23[a]
C1		354, 463, 535	751	1.69	0.033
C2		319, 492, 536	759	1.67	0.027
(NND)$_2$-azaBODIPY		351, 600, 750	813	1.59	0.019
(TPA)$_2$-azaBODIPY		366, 591, 742	777	1.63	0.018
(PTZ)$_2$-azaBODIPY		363, 575, 740	773	1.64	0.0007

[a]-from Ref. [30]

Considerable red-shift in the fluorescence emission was also witnessed. At the excitation of azaBODIPY absorption peak maxima, the fluorescence emission of **azaBODIPY** in benzonitrile, located at 702 nm, was red-shifted to 751 and 762 nm in **C1** and **C2**. However, in the push-pull

systems, the emission was quantitatively quenched. Interestingly, in DCB and toluene, although such a trend with respect to substitution was observed, the quenching was only nearly 50% in the case of **(NND)$_2$-azaBODIPY** and **(TPA)$_2$-azaBODIPY** push-pull systems (slightly more in DCB), however, it was over 96% for **(PTZ)$_2$-azaBODIPY**. These results indicate the significance of the nature of donors and solvents in governing the fluorescence properties of the investigated push-pull systems. The measured fluorescence quantum yields (Φ_f) are also listed in Table 1. Substantially lower Φ_f for **C1** and **C2** compared to **azaBODIPY**, and almost zero for the push-pull systems in benzonitrile were noted. The singlet excited energy was calculated from the average energy of the low energy absorption and fluorescence peak and was found to be ~1.67 eV

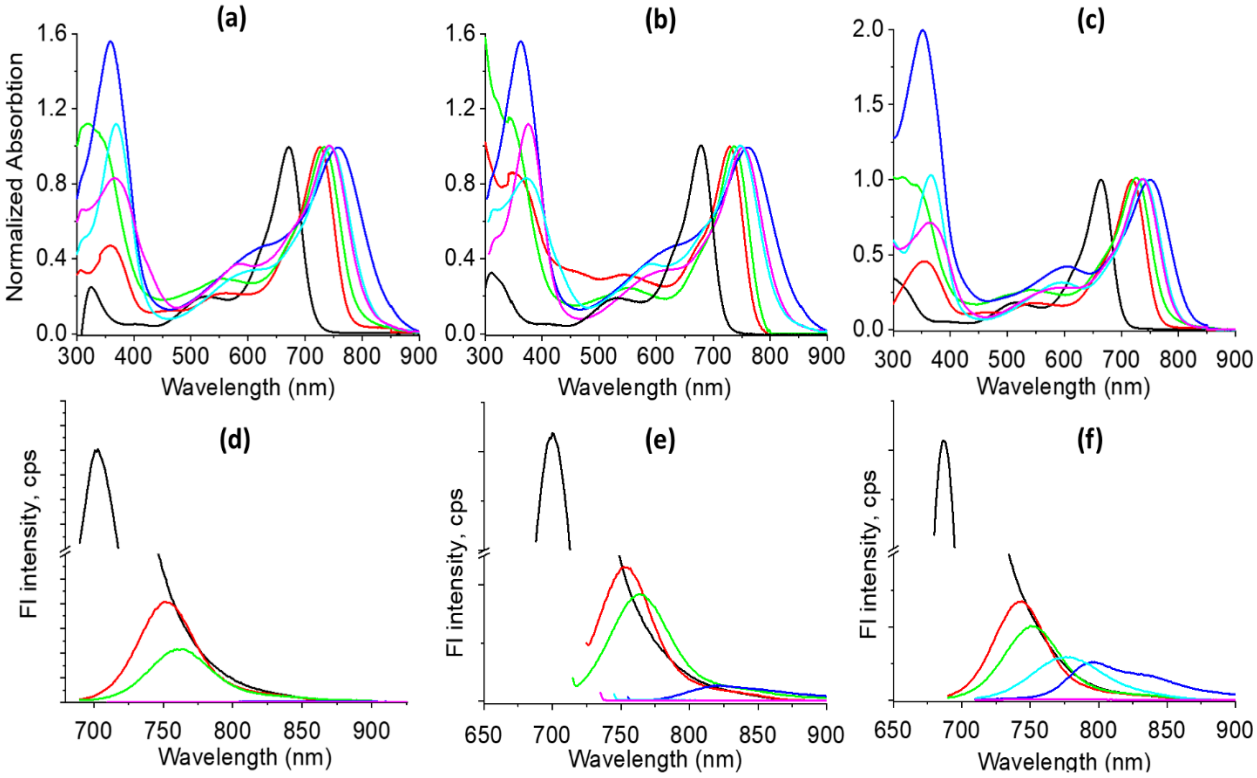

Figure 2. Absorption (a, b and c) fluorescence (d, e and f) spectrum of **azaBODIPY** (black), **C1** (red), **C2** (green), **(NND)$_2$-azaBODIPY** (blue), **(TPA)$_2$-azaBODIPY** (light blue), and **(PTZ)$_2$-azaBODIPY** (magenta) in benzonitrile (a and d), DCB (b and e), and toluene (c and f). Samples were excited at the far-red peak listed in Table 1.

which was about 0.13 eV lower than that of pristine azaBODIPY, being 1.80 eV. The triplet energy of **azaBODIPY** reported earlier is about 0.92 eV.[32,36] The fluorescence lifetime determined from

the time-correlated single photon counting technique resulted in a lifetime of ~4 ns for **azaBODIPY** that was substantially lower in **C1** and **C2** ranging between 0.7–1.5 ns depending upon the solvent. For the push-pull systems, due to low emissions, no reliable data could be secured.

Fluorescence studies were also performed by exciting the samples corresponding to the absorption peak maxima of the nitrogenous donors. As shown in Figure S23, in benzonitrile, pristine TPA and PTZ revealed absorption peak maxima at 330 and 370 nm, respectively. In the push-pull systems, they revealed minor changes due to linkage and overlap of azaBODIPY absorption in this region. Fluorescence peak maxima of TPA and PTZ were located at 405 and 488 nm, respectively. Interestingly, in the push-pull systems, these emissions were quenched over 95% with no new peaks in the region of azaBODIPY emission suggesting that the quenching is likely not due to energy transfer. Such a trend was also observed in toluene; however, the quenching was ~80%. The solvent polarity dependent quenching suggests it is due to charge transfer type interactions.[8]

As the redox potentials of the donor and acceptor take up a key role in governing the free-energy changes for electron transfer reactions, electrochemical studies using both differential pulse voltammetry (DPV) and cyclic voltammetry (CV) were performed in benzonitrile. Figure 3 shows the DPVs of the compounds, while Table 2 lists redox potential along with the calculated free-energy values for charge separation and recombination. The first reduction and first oxidation of **C1** were located at -0.22 and 1.27 V vs. Ag/AgCl while that of **C2** these values were at -0.27 and 1.20 V resulting in an electrochemical redox gap of 1.47 to 1.49 V which was about 0.20 V smaller than that calculated from optical data (see $E_{0,0}$ values in Table 1). Importantly, the facile reduction of azaBODIPY in **C1** and **C2** was borne out. The presence of donor entities in the push-pull systems revealed additional oxidation waves and they appeared prior to the oxidation process of the azaBODIPY entity. Owing to the presence of two donor entities in each push-pull system, the peak currents were roughly twice as much of the first reduction of the azaBODIPY entity of a given push-pull system. Oxidation of NND, TPA, and PTZ entities of the push-pull systems appeared at 0.85, 1.05 and 0.78 V, facile oxidation of PTZ compared to the other two donors was clear from this study. Unlike the reversible azaBODIPY first reduction, the oxidation process of the donor entities in the push-pull systems was quasi-reversible.

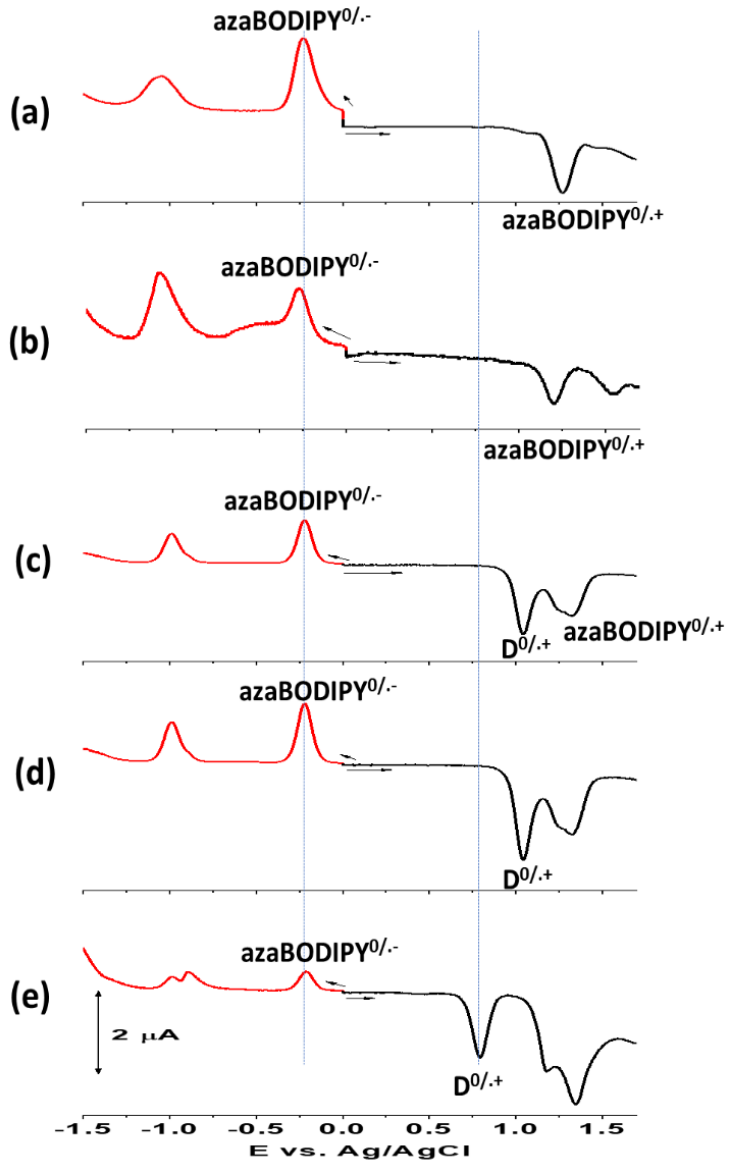

Figure 3. Differential pulse voltammograms of (a) **C1**, (b) **C2** (c) **(NND)$_2$-azaBODIPY** (d) **(TPA)$_2$-azaBODIPY**, and (e) **(PTZ)$_2$-azaBODIPY** in benzonitrile containing 0.1 M (TBA)ClO_4.

Table 2. Electrochemical redox potentials and free-energy changes associated with light-induced electron transfer of the push-pull systems.

Compound	Reduction, V vs. Ag/AgCl	Oxidation, V vs. Ag/AgCl	ΔG_s, eV	ΔG_{CS}, eV	ΔG_{CR}, eV
C1	-1.06, -0.22	1.27	--	--	--
C2	-1.06, -0.27	1.20	--	--	--
(NND)$_2$-azaBODIPY	-1.02, -0.25	0.85,[a] 1.10	-0.094	-0.26	-1.36
(TPA)$_2$-azaBODIPY	-0.99, -0.21	1.05,[a] 1.25	-0.086	-0.24	-1.37
(PTZ)$_2$-azaBODIPY	-0.89, -0.21	0.78,[a] 1,19	-0.086	-0.32	-1.31

[a] - Oxidation corresponding to the Donor entity.

[b]- Estimated error in values = ±5%

Frontier orbitals of the investigated compounds on B3LYP/6-31G(d, p) optimized structures[57] are shown in Figure 4. For **C1** and **C2** having no donor entities, the HOMO was distributed all over the molecule including the phenyl-acetylene linkers (see Figure 4a for **C2**), however, the HOMO-1 was more on the phenyl-acetylene linkers. The LUMO was mainly on the azaBODIPY part with considerable coefficients on the thiophene entities while the LUMO+1 were distributed on the entire molecule without appreciable coefficients on the thiophene entities. Having two donor entities on the azaBODIPY revealed notable changes (Figure 4b to d). In all three push-pull systems, the HOMO was distributed on the entire molecule including the donor entities but without contributions to the thiophene entities. Interestingly, the HOMO-1 was localized symmetrically on the acetylene-donor part of the push-pull systems. The LUMO of the push-pull systems was on the azaBODIPY entity with contributions on the thiophene units while LUMO+1 were on the azaBODIPY-acetylene part of the molecules. A charge transfer from HOMO → LUMO or HOMO-1 → LUMO could be envisioned from the location of the frontier orbitals.

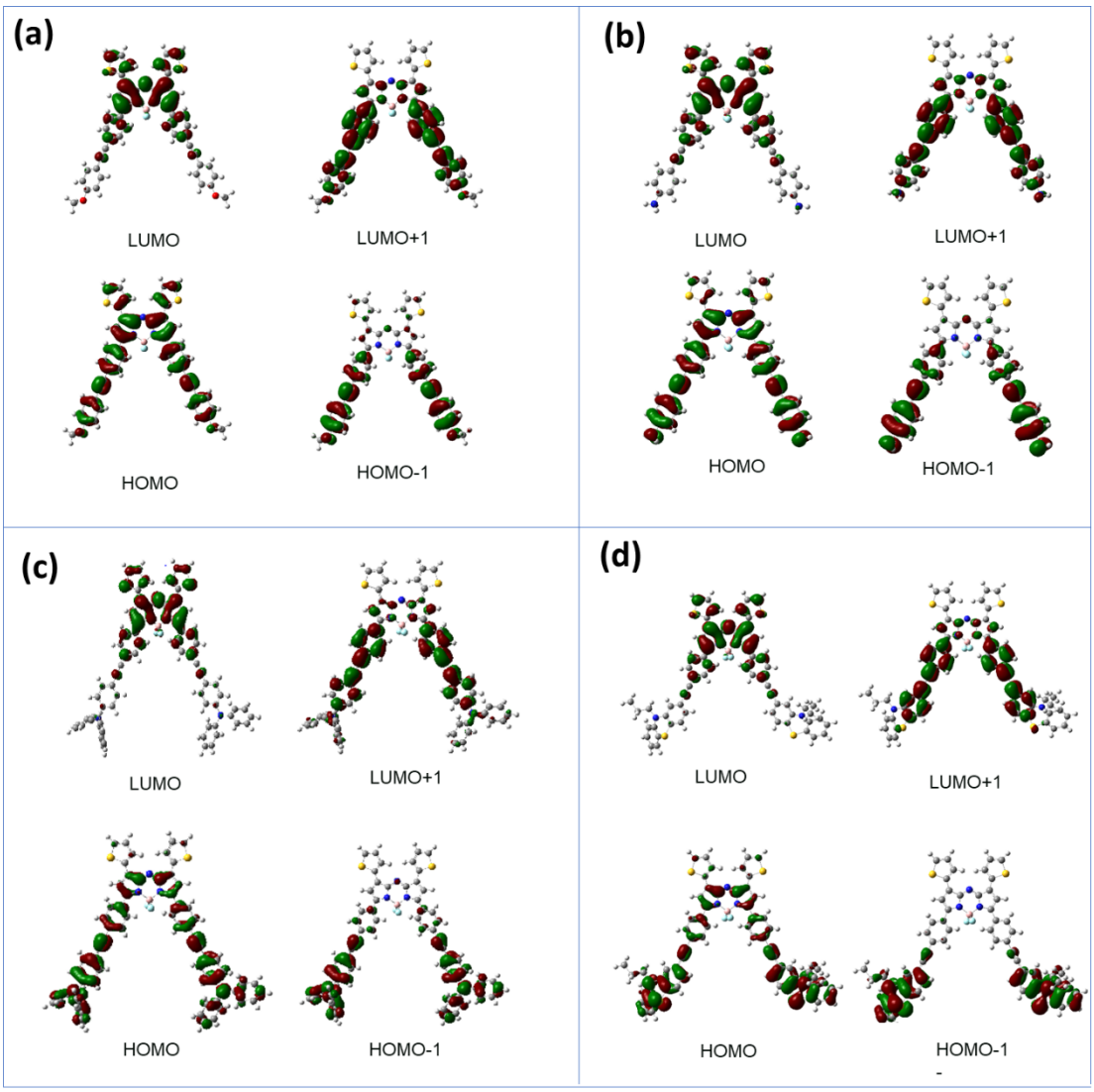

Figure 4. Frontier orbitals on B3LYP/6-31G(d, p) optimized structures of (a) **C2** (b) **(NND)$_2$-azaBODIPY**, (c) **(TPA)$_2$-azaBODIPY**, and (d) **(PTZ)$_2$-azaBODIPY**.

The redox potentials are used in combination with optical data to estimate the energies of the radical ion pair states (E_{CS}) and free energy change for the charge separation (ΔG_{CS}) by using the equations 1–3,[58]

$$E_{CS} = e[E_{1/2}(D^{+\cdot}/D) - E_{1/2}(A/A^{-\cdot})] + G_S \qquad (1)$$

$$\Delta G_{CS} = E_{CS} - E_{0-0} \qquad (2)$$

where $E_{1/2}(D^{\cdot+}/D)$ is the first oxidation potential of the donor, $E_{1/2}(A/A^{\cdot-})$ is the first reduction potential of the acceptor and G_S is the ion-pair stabilization energy,

$$G_S = \frac{-e^2}{4\pi\varepsilon_0\varepsilon_S R_{D-A}} \quad (3)$$

where $R_{D\text{-}A}$ is the center-to-center distance between the donor and acceptor, ε_S is the dielectric constant of the solvent used for the optical and redox studies, in this case benzonitrile. The lowest excited singlet state energy ($E_{0\text{-}0}$) is estimated from the crossing point of absorption and fluorescence spectra as listed in Table 1.

The estimated free-energy values listed in Table 2 reveal that reductive electron transfer (excited molecule accepting an electron) is indeed possible in these push-pull systems from one of the Donor entities to the single excited azaBODIPY. Energy level diagrams were subsequently established using the information discussed in the above paragraphs and such diagrams are shown in Figure 5. For **C1** and **C2**, a simple scheme could be envisioned, that is, excitation of azaBODIPY corresponding to its singlet state (low energy absorption peak maxima in Table 1) would produce ^{1}azaBODIPY*. The ^{1}azaBODIPY* thus produced could emit from the singlet excited state (radiative fluorescence) or undergo nonradiative energy loss (thermal), or in part undergo intersystem crossing (ISC) to populate the triplet state. The ^{3}azaBODIPY* would eventually return to the ground state via the process of phosphorescence (Figure 5a).

Interestingly, in the case of the push-pull systems where efficient fluorescence quenching was observed, deactivation of ^{1}azaBODIPY* *via* radiative emission is going to a minor process, and as charge separation is thermodynamically feasible, ^{1}azaBODIPY* could undergo reductive electron transfer by abstracting an electron from one of the donor entities to the half-filled HOMO (or HOMO-1) orbital, resulting in $D^{\cdot+}$-azaBODIPY$^{\cdot-}$ (D = NND, TPA, or PTZ) charge separated states. As the entities in the push-pull system are coupled, an intermediate charge transfer state, $D^{\delta+}$-azaBODIPY$^{\delta-}$, prior to the solvated charge-separated state could also be envisioned. The charge-separated state could return to the ground state directly by the process of charge recombination either radiatively via the process of charge recombination emission or nonradiatively. Alternatively, this state could populate the low-lying ^{3}azaBODIPY* (E_T ~ 1.0 eV). The newly formed ^{3}azaBODIPY* would return to the ground state via phosphorescence or by nonradiative mechanism. As no charge recombination emission was observed in benzonitrile for the investigated push-pull systems, the latter mechanism of populating the ^{3}azaBODIPY* could be considered a more likely path (Figure 5b). In nonpolar toluene, a complete charge separation is not

expected due to high solvation energy demand, however, a partial charge transfer could occur as is supported by fluorescence quenching observed for these push-pull systems in toluene.

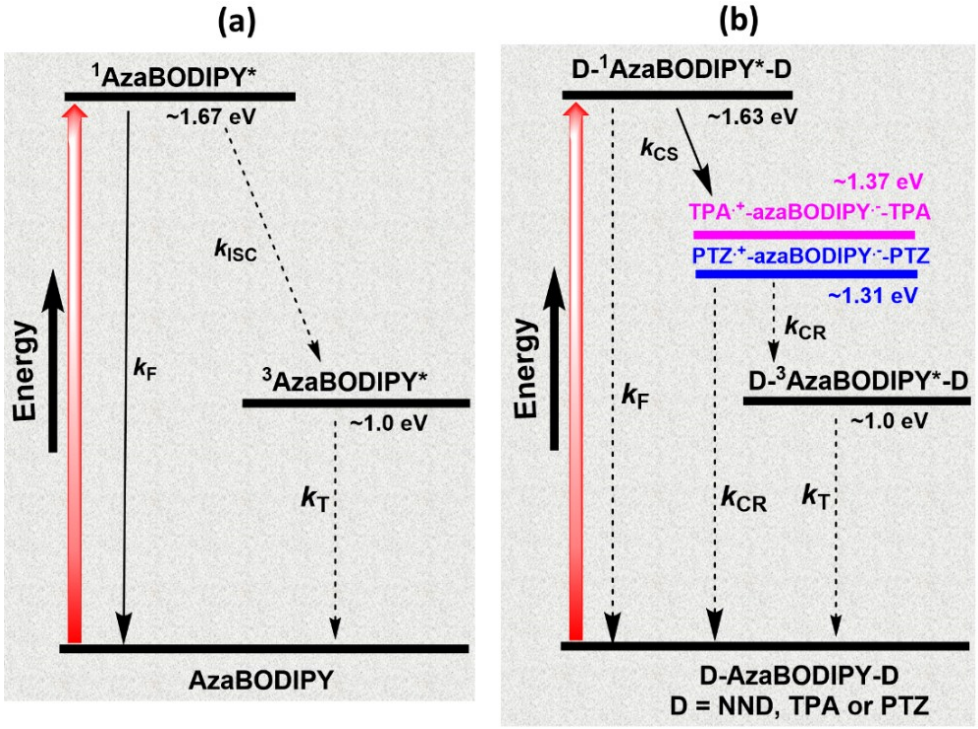

Figure 5. Jablonski type energy level diagram for the (a) control **azaBODIPY** and (b) push-pull systems in benzonitrile. Solid line – most likely process, dashed line-less likely process. Abbreviations: CS = charge separation, ISC = intersystem crossing, F = fluorescence emission, T = triplet emission, and CR = charge recombination.

Spectroelectrochemical studies were subsequently performed to characterize the one-electron reduced and one-electron oxidized products of the investigated compounds, as shown in Figure 6. For each process a potential 100 mV past the peak potential was applied and the spectra were recorded until no additional changes were observed. During the process of first reduction of control azaBODIPY (**C2**), intensity decrease of the original peaks was associated with new peaks 456, 524, and 918 nm. Isosbestic points at 388 and 783 nm were also observed. Conversely, during the first oxidation process, a decrease in intensity of the original peaks did not result in new peaks, only an increase in intensity in the 300–320 nm range was observed. For the push-pull systems, the spectral trends were almost similar but with slightly red-shifted peaks. For example, for **(TPA)$_2$-azaBODIPY**, new peaks of one-electron reduced product were located at 491, 533 and 924 nm, however, no new peaks were observed during the process of one-electron oxidation except

for a blue-shift of 10 nm in the case of **(TPA)$_2$-azaBODIPY** for the high-energy UV-band corresponding to the TPA donor entities was observed. It is important to note that although the oxidation is mainly donor-centered, the reduction in azaBODIPY peaks suggest strong electronic coupling between them, as suggested by the distribution of the HOMO orbitals.

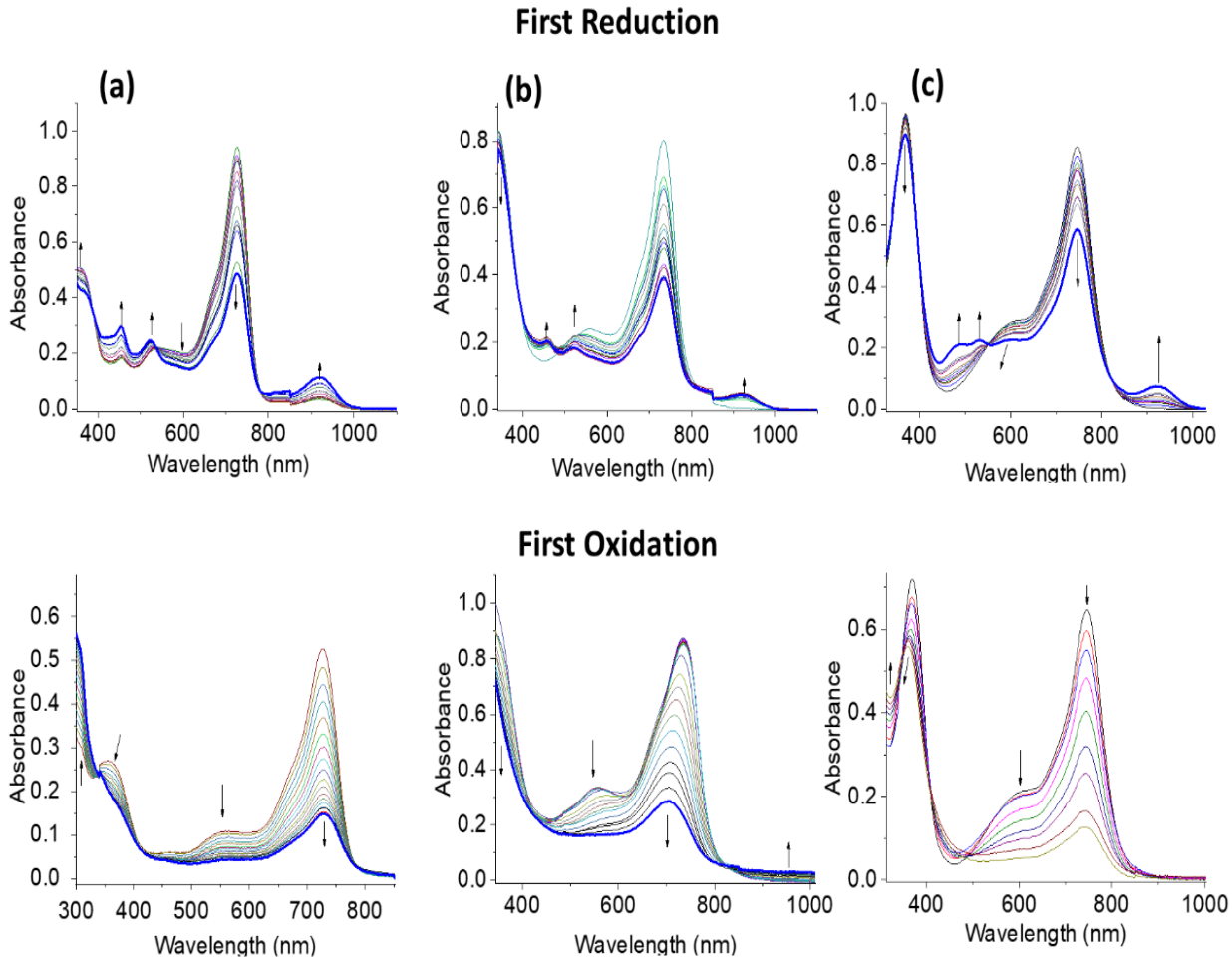

Figure 6. Spectral changes during first reduction (top) and first oxidation (bottom) of (a) **C1**, (b) **(NND)$_2$-azaBODIPY** and **(TPA)$_2$-azaBODIPY** in benzonitrile containing 0.2 M (TBA)ClO_4.

Finally, pump-probe studies were performed to probe photodynamics and secure evidence of charge separation in the push-pull systems. Figure 7a shows the femtosecond transient absorption (fs-TA) spectra at the indicated delay times of control **azaBODIPY**, **C2** in benzonitrile. The instantaneously formed ^{1}azaBODIPY* revealed excited state absorption bands at 438, 580, and 1080 nm. In addition, negative peaks at 535, 663 and 738 nm were observed. By comparison with the absorption and fluorescence, the first two peaks are attributed to the ground state bleaching (GSB) and the latter to stimulated emission (SE). Decay of the positive peaks and recovery of the negative peaks started slowly developing new peaks around 625, 678 and 830 nm that could be attributed to ^{3}azaBODIPY* although such a process was not complete within the delay time window of 3 ns.

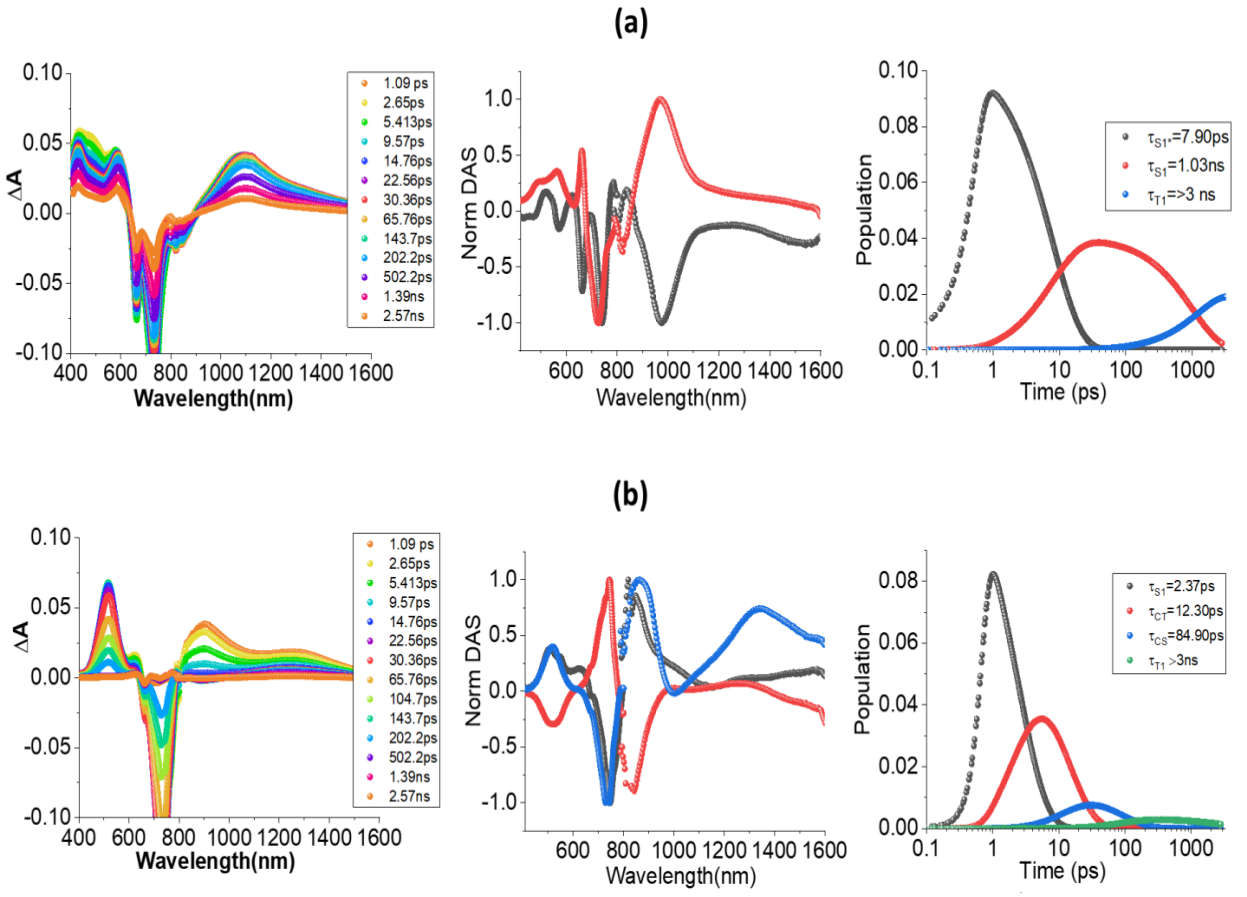

Figure 7. Fs-TA spectra at the indicated delay times of (a) **C2** and (b) **(PTZ)$_2$-azaBODIPY** in benzonitrile at the excitation wavelength of 668 nm. The decay associated spectra and population time profiles from GloTarAn analysis are shown in the middle and right-hand panels, respectively. The DAS of T_1 state is not shown for clarity.

The data was further analyzed using Global Target Analysis (Glotaran) program.[59] A three-component fit, representing $S_0 \rightarrow S_1 \rightarrow T_1$ was adopted. The decay associated spectra (DAS) are shown in Figure 7a middle panel were good complementarity between the two singlet states was apparent. Time constants of 7.9 ps for $S_0 \rightarrow S_1$ population and 1.03 ns for the S_1 state were obtained (Figure 7a right-hand panel). The S_1 lifetime agreed well with the earlier discussed lifetime from the TCSPC technique. A third component with a lifetime > 3 ns was also observed. Nanosecond transient absorption (ns-TA) spectral studies resulted in weak/noisy spectra from where the time constant for the triplet state was difficult to arrive.

Table 3. Kinetic values for different photo events of the studies systems.[a]

Compound	Solvent	τ_{rise}, ps	τ_{S1}, ps	τ_{CT}, ps	τ_{CS}, ps
C1	PhCN	7.90	1000	--	--
C2		6.33	998	--	--
$(NND)_2$-azaBODIPY		--	4.23	16.99	194.5
$(TPA)_2$-azaBODIPY		--	3.55	9.51	49.99
$(PTZ)_2$-azaBODIPY		--	2.37	12.30	84.90
C1	Toluene	7.72	1060	--	--
C2		6.53	1100	--	--
$(NND)_2$-azaBODIPY		--	5.97	265.4	--
$(TPA)_2$-azaBODIPY		--	3.74	30.3	--
$(PTZ)_2$-azaBODIPY		--	3.10	90.3	--

[a]-estimated error = ±10%

Figure 7b shows the fs-TA spectra at the indicated delay times **$(PTZ)_2$-azaBODIPY** in benzonitrile. At the earliest delay time of 1–2 ps, peaks corresponding to both S_1 and CT state were visible. ESA peaks at 500, 900 and 1317 nm were observed. In addition, negative peaks at 663 and 744 nm, corresponding to GSB and SE were observed. During the next 30 ps, the positive ESA peaks experienced a small spectral shift, that is, the 900 nm peak shifted to 890 nm and the 1317 nm peak moved to 1346 nm, likely to the transformation of CT → CS was observed. In the next 30–100 ps range, new peaks started emerging at 626, 678 and 826 nm, attributable to the CS

state populating the triplet state. Glotaran analysis of the data by fitting S_1 → CT → CS → T_1 state is shown in Figure 7b middle panel. Good complementarity for the conversion of CT → CS (inverse of the peaks between the two states) was observed. The derived time constants were found to be 12.3 ps for the CT state and 84.9 ps for CS (Figure 7b right-hand panel).

As shown in Figure 8, fs-TA spectral features of the push-pull systems **(NND)$_2$-azaBODIPY** and **(TPA)$_2$-azaBODIPY** closely resembled that of **(PTZ)$_2$-azaBODIPY**. These results conclusively prove charge separation in the push-pull systems. Time constants for the different processes from Glotaran analysis are summarized in Table 3 below. In all, the CS state lasted between 50–200 ps depending on the nature of the Donor entity suggesting charge stabilization to some extent in these push-pull systems in benzonitrile.

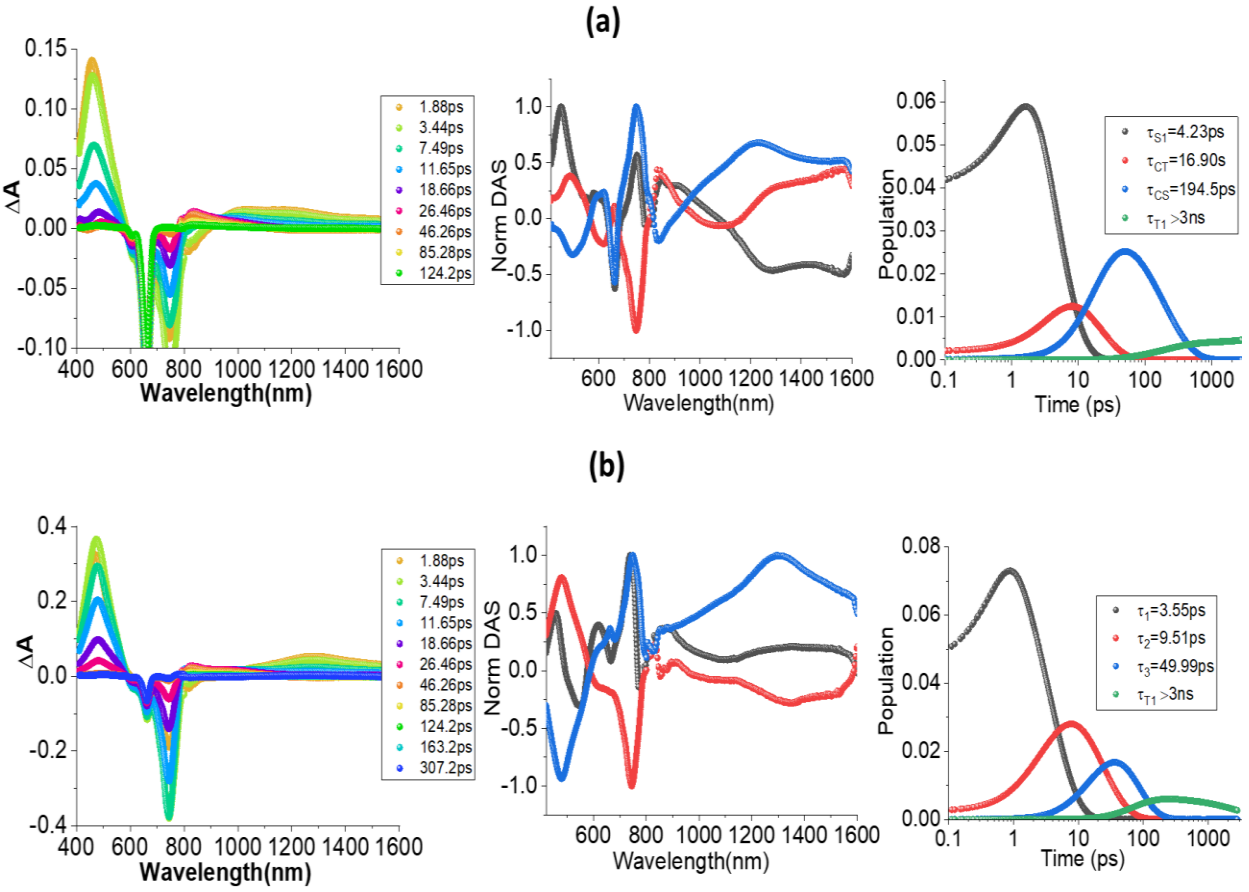

Figure 8. Fs-TA spectra at the indicated delay times of (a) **(NND)$_2$-azaBODIPY** and (b) **(TPA)$_2$-azaBODIPY** in benzonitrile at the excitation wavelength of 668 nm. The decay associated spectra and population time profiles from GloTarAn analysis is shown in the middle and right-hand panels, respectively. The DAS of T_1 state is not shown for clarity.

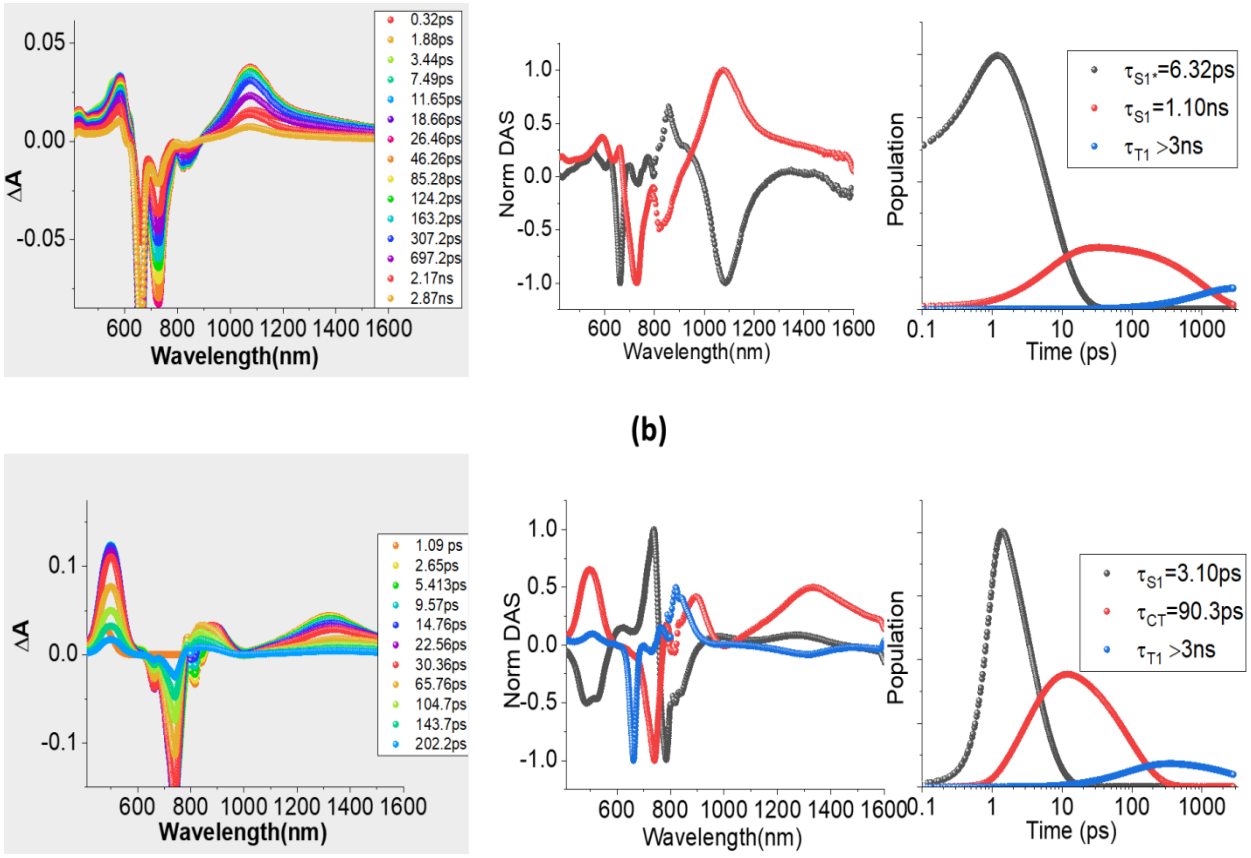

Figure 9. Fs-TA spectra at the indicated delay times of (a) **C2** and (b) **(PTZ)$_2$-azaBODIPY** in toluene at the excitation wavelength of 668 nm. The decay associated spectra and population time profiles from GloTarAn analysis is shown in the middle and right-hand panels, respectively. The DAS of T_1 state is not shown for clarity.

The photophysical properties were also monitored in toluene as charge transfer was predicted for the push-pull systems due to substantial lowering of their fluorescence quantum yields (Table 1). Figure 9a shows the fs-TA spectra at the indicated delay times for control **C2**. Overall, the spectral features were similar to that observed in benzonitrile. Time constants for the different events were evaluated by Glotaran analysis of the data by fitting $S_0 \rightarrow S_1 \rightarrow T_1 \rightarrow$ GS model (Figure 9b middle panel and right-hand panel) and the results are given in Table 3. The time constants for S_1 state agreed well with lifetimes determined from the TCSPC technique.

Fs-TA results obtained for **(PTZ)$_2$-azaBODIPY** is shown in Figure 9b. Immediately after excitation, the spectrum recorded at a delay time of 1 ps revealed ESA peaks at 502, 898, and 1323 nm. In addition, GSB peaks at 660 nm and SE peaks at 744 nm were observed. The ESA peaks at

502 and 898 nm had features of $PTZ^{\delta+}$-azaBODIPY$^{\delta-}$ charge transfer state suggesting its ultrafast occurrence from the initially formed ^{1}azaBODIPY*. Decay and recovery of the positive and negative peaks revealed another set of new peaks at 683 and 827 nm expected for ^{3}azaBODIPY*. The data was further subjected to Glotaran analysis by providing two kinetic paths, viz,: $S_o \rightarrow S_1 \rightarrow CT \rightarrow CS \rightarrow GS$ and $S_o \rightarrow S_1 \rightarrow CT \rightarrow GS$. The last one is without the charge separated state. As shown in Figure 9b middle panel, the best fit was the latter model. This is reasonable since formation of fully charge separated state, $PTZ^{\cdot+}$-azaBODIPY$^{\cdot-}$, in the nonpolar solvent is unlikely due to the high solvation energy requirement. The time constant for the CT state was about 90 ps (see Figure 9b right-hand panel).

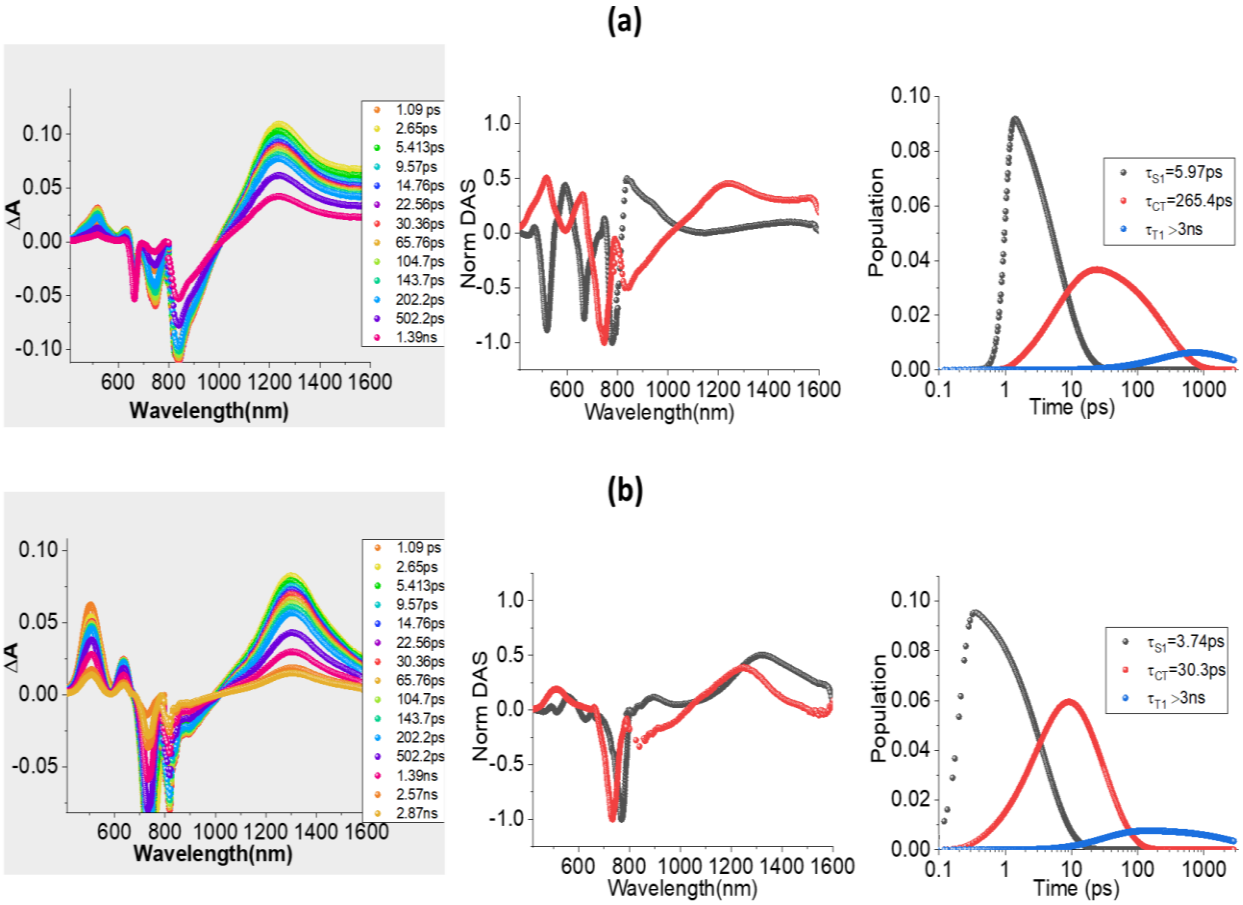

Figure 10. Fs-TA spectra at the indicated delay times of (a) **(NND)$_2$-azaBODIPY** and (b) **(TPA)$_2$-azaBODIPY** in toluene at the excitation wavelength of 668 nm. The decay associated spectra and population time profiles from GloTarAn analysis is shown in the middle and right-hand panels, respectively. The DAS of T_1 state is not shown for clarity.

For the next two push-pull systems, **(NND)$_2$-azaBODIPY** and **(TPA)$_2$-azaBODIPY**, transient spectral features revealed features of charge transfer, however, not as well developed as that of **(PTZ)$_2$-azaBODIPY** (Figure 10). In these cases, although the 500 nm peak corresponding to the charge transfer state was present, the 900 nm peak appeared as only a shoulder peak. Glotaran analysis was subsequently performed by fitting the data to the $S_o \rightarrow S_1 \rightarrow CT \rightarrow GS$ model and the time constants are listed in Table 3. The CT states persisted more in the case of **(NND)$_2$-azaBODIPY** compared to **(TPA)$_2$-azaBODIPY**

Summary

The newly synthesized donor-acceptor push-pull systems featuring far-red absorbing sensitizer azaBODIPY as a photosensitizer-electron acceptor along with nitrogenous electron donors *N,N*-dimethylaniline, triphenylamine, and phenothiazine revealed several interesting features with regard to their excited state electron transfer properties. Using a range of physico-chemical techniques, it was possible to arrive at the structure of these push-pull systems. The measured redox potentials revealed facile reduction of azaBODIPY and facile oxidation of nitrogenous donors and the performed spectroelectrochemical studies revealed diagnostic peaks of azaBODIPY$^{\bullet-}$ in the visible and near-IR regions. Further, free-energy calculations indicated charge separation from one of the donor entities to the ^{1}azaBODIPY* to yield charge-separated states in a polar solvent but only partial charge transfer in toluene. The fluorescence emission of ^{1}azaBODIPY* and calculated quantum yields revealed a different level of quenching depending upon the nature of the solvent and donor entities. Fs-TA studies confirmed the occurrence of charge separation in benzonitrile and kinetic analysis performed by GloTarAn analysis revealed the charge-separated states to last about 50–200 ps depending on the nature of the donor. Finally, the charge transfer states in toluene and charge-separated states in benzonitrile populated the low-lying ^{3}azaBODIPY* prior to returning the push-pull system to the ground state.

Experimental section

General methods

All the chemicals were used as received, unless otherwise indicated. The reactions that were sensitive to oxygen or moisture were carried out using the standard schlenk method under a nitrogen/argon atmosphere. The chemicals were purchased from commercial sources and used

without further purification. The ^{1}H NMR (400 MHz) and ^{13}C NMR (100 MHz) spectra were obtained on a Bruker Avance (III) 400 MHz spectrometer, using $CDCl_3$ as the solvent, and chemical shifts were reported in parts per million (ppm). The residual proton (δ = 7.26 ppm) and ^{13}C (δ = 77.0 ppm) spectra in $CDCl_3$ were recorded using tetramethylsilane (TMS) as an internal reference. At IIT-I, UV-visible absorption spectra of all compounds in dichloromethane were measured on a Carry-100 Bio UV-visible spectrophotometer. HRMS was recorded on a Bruker-Daltonics micro TOF-Q II mass spectrometer.

UV-visible spectra were measured using a Jasco UV-visible-near IR spectrophotometer. Fluorescence and phosphorescence spectra were obtained with a Horiba Yvon Nanolog coupled with time-correlated single-photon counting and nanoLED excitation sources, using a right-angle detection method. Differential pulse and cyclic voltammograms were taken with an EG&G 263A electrochemical analyzer, using a three-electrode system with a platinum button electrode as the working electrode, a platinum wire as the counter electrode, and an Ag/AgCl electrode as the reference electrode. The internal standard was the ferrocene/ferrocenium redox couple, and all solutions were purged with argon gas prior to electrochemical and spectral measurements. Spectroelectrochemical studies were conducted using a SEC-C cell assembly provided by ALS Co., Ltd. (Tokyo, Japan). This cell had a Pt counter electrode, a 6 mm Pt Gauze working electrode, and an Ag/AgCl reference electrode in a 1.0 mm path length quartz cell, with an optical transmission limited to 6 mm over the surface of the Pt Gauze working electrode.

An Ultrafast Femtosecond Laser Source (Libra) by Coherent was utilized to perform femtosecond transient absorption spectroscopy experiments, incorporating a diode-pumped, modelocked Ti:sapphire laser (Vitesse) and a diode-pumped intracavity doubled Nd:YLF laser (Evolution) to generate a compressed laser output of 1.45 W. For optical detection, a Helios transient absorption spectrometer coupled with an Ultrafast Systems LLC supplied femtosecond harmonics generator was employed. The sources for the pump and probe pulses were derived from Libra's fundamental output (Compressed output 1.45 W, pulse width 100 fs) at a repetition rate of 1 kHz; 95% of the laser's fundamental output was introduced into a TOPAS-Prime-OPA system with a 290−2600 nm tuning range from Altos Photonics Inc., (Bozeman, MT), while the rest of the output was used to generate a white light continuum. Data was collated from kinetic traces at the appropriate wavelengths, and later analyzed using Ultrafast Systems' Surface Xplorer software.

All measurements were conducted in degassed solutions at 298 K. The rate constants are reported with an estimated error margin of ±10%.

Synthesis of C1:

In 100 ml round bottom flask, di-bromo aza-BODIPY **1** (0.500 g, 0.75 mmol), ethynylbenzene (0.153 g, 1.50 mmol) were dissolved in a THF/TEA mixture (v/v,1:1) and the solution was degassed with argon for 10 minutes. To this reaction mixture $Pd(PPh_3)_4$ (0.050 g), CuI (0.007 g) were added. After stirring 12 hrs at 60 °C, the solvent was removed under vacuum and the product was purified by column chromatography using neutral activated aluminum oxide (1: 1 DCM : Hexane) as an eluent to yield 0.453 g (85%) of **C1**. **^{1}H NMR** (400 MHz, $CDCl_3$, δ in ppm): 8.06-8.02 (4H, m), 7.95-7.94 (2H, d, J = 4Hz), 7.89-7.87 ((1H, d, J = 8Hz), 7.64-7.55 (10H, m), 7.37-7.36 (5H, m), 7.22-7.20 (2H, d, J = 4Hz), 6.97 (2H, s). **^{13}C NMR** (100 MHz, $CDCl_3$, δ in ppm): 158.3, 145.3, 138.3, 135.3, 135.2, 134.6, 132.2, 132.1, 131.9, 131.8, 131.7, 131.0, 130.6, 130.5, 130.4, 130.2, 130.0, 129.8, 129.5, 128.6, 128.4, 128.3, 127.7, 127.6, 126.0, 125.7, 123.0, 116.8, 92.5, 89.4. **^{11}B NMR** (160 MHz, $CDCl_3$) δ 0.91 (t, $J_{B\text{-}F}$ = 30.9 Hz). **^{19}F NMR** (471 MHz, $CDCl_3$) δ -130.42 (q, $J_{F\text{-}B}$ = 31.1 Hz). **HRMS** (ESI) *m/z*: $[M + H]^+$ calcd for $C_{44}H_{27}BF_2N_3S_2$: 710.1703; found 710.1709.

Synthesis of C2:

In 100 ml round bottom flask, di-bromo aza-BODIPY **1** (0.500 g, 0.75 mmol), 1-ethynyl-4-methoxybenzene (0.199 g (1.50 mmol) were dissolved in a THF/TEA mixture (v/v,1:1) and the solution was degassed with argon for 10 minutes. To this reaction mixture $Pd(PPh_3)_4$ (0.050 g), CuI (0.007 g) were added. After stirring 12 hrs at 60 °C, the solvent was removed under vacuum and the product was purified by column chromatography using neutral activated aluminum oxide (1: 1 DCM : Hexane) as an eluent to yield 0.462 g (80%) **C2**. **^{1}H NMR** (400 MHz, $CDCl_3$, δ in ppm): 8.04-8.02 (4H, d, J = 8Hz), 7.93 (2H, s), 7.60-7.57 (6H, m), 7.51-7.48 (4H, d, J = 12Hz), 7.26 (2H, s), 6.96 (2H, s), 6.90-6.88 (4H, d, , J = 8Hz), 3.84 (6H, s); **^{13}C NMR** (100 MHz, $CDCl_3$, δ in ppm): 159.9, 158.3, 149.3, 145.3, 138.2, 134.7, 133.3, 131.5, 130.6, 130.3, 129.8, 129.5, 128.3, 126.4, 116.8, 115.1, 114.1, 92.7, 88.3, 55.3. **^{11}B NMR** (160 MHz, $CDCl_3$) δ 0.92 (t, $J_{B\text{-}F}$ = 30.9 Hz). **^{19}F NMR** (471 MHz, $CDCl_3$) δ -130.46 (t, $J_{F\text{-}B}$ = 31.0 Hz). **HRMS** (ESI) *m/z*: $[M]^+$ calcd for $C_{46}H_{30}BF_2N_3S_2O_2$: 769.1844; found 769.1843.

Synthesis of (NND)$_2$-azaBODIPY:

In 100 ml round bottom flask, di-bromo aza-BODIPY **1** (0.500 g, 0.75 mmol), 4-ethynyl-*N*, *N*-dimethylaniline (0.218 g, 1.50 mmol) were dissolved in a THF/TEA mixture (v/v,1:1) and the solution was degassed with argon for 10 minutes. To this reaction mixture $Pd(PPh_3)_4$ (0.050 g), CuI (0.007 g) were added. After stirring 12 hrs at 60 °C, the solvent was removed under vacuum and the product was purified by column chromatography using neutral activated aluminium oxide (1: 1 DCM : Hexane) as an eluent to yield 0.451 g (75%) **(NND)$_2$-azaBODIPY**. **^{1}H NMR** (400 MHz, $CDCl_3$, δ in ppm): 8.05-8.03 (4H, J = 8Hz), 7.94-7.93 (2H,d, J = 4Hz), 7.59-7.57 (6H, d, J = 8Hz), 7.45-7.42 (4H, d, J = 12Hz), 7.22-7.20 (2H, t, J = 4Hz), 6.98 (2H, s), 6.68-6.66 (4H,d, J = 8Hz), 3.01 (12H, s). **^{13}C NMR** (100 MHz, $CDCl_3$, δ in ppm): 158.2, 150.3, 145.3, 134.8, 133.0, 131.3, 130.1, 129.6, 129.5, 128.3, 127.1, 116.9, 111.8, 109.7, 94.5, 88.0. **^{11}B NMR** (160 MHz, CDCl3) δ 0.96 (t, $J_{B\text{-}F}$ = 31.0 Hz). **^{19}F NMR** (471 MHz, $CDCl_3$) δ -130.57 (q, $J_{F\text{-}B}$ = 31.1 Hz). **HRMS** (ESI) *m/z*: $[M + H]^+$ calcd for $C_{48}H_{37}BF_2N_5S_2$: 796.2599; found 796.2554.

Synthesis of (TPA)$_2$-azaBODIPY:

Synthesis of **(TPA)$_2$-azaBODIPY** is given elsewhere.[43].

^{11}B NMR (160 MHz, $CDCl_3$) δ 1.12-0.73 (t, $J_{B\text{-}F}$ = 30.9 Hz). **^{19}F NMR (**471 MHz, $CDCl_3$) δ -130.50 (q, $J_{F\text{-}B}$ = 31.0 Hz).

Synthesis of (PTZ)$_2$-azaBODIPY:

In 100 ml round bottom flask, di-bromo aza-BODIPY **1** (0.500 g, 0.75 mmol), 3-ethynyl-10-propyl-10H-phenothiazine (0.399 g, 1.50 mmol) were dissolved in a THF/TEA mixture (v/v,1:1) and the solution was degassed with argon for 10 minutes. To this reaction mixture $Pd(PPh_3)_4$ (0.050 g), CuI (0.007 g) were added. After stirring 12 hrs at 60 °C, the solvent was removed under vacuum and the product was purified by column chromatography using neutral activated aluminium oxide (1: 1 DCM : Hexane) as an eluent to yield 0.600 g (77%) **(PTZ)$_2$-azaBODIPY**. **^{1}H NMR** (400 MHz, $CDCl_3$, δ in ppm): 8.04-8.02 (4H, d, J = 8 Hz), 7.94 (2H, s), 7.59-7.57 (6H, d, J = 8 Hz), 7.34-7.30 (4H, m), 7.22-7.11 (6H, m), 6.96-6.79 (8H, m), 3.84-3.81 (4H, t, J = 8 Hz), 1.86-1.81 (4H, q), 1.04-1.00 (6H, t, J = 8 Hz). **^{13}C NMR** (100 MHz, $CDCl_3$, δ in ppm): 158.2, 145.6, 145.3, 144.5, 138.1, 134.7, 131.5, 131.0, 130.7, 130.3, 130.3, 129.8, 129.5, 128.3, 127.5, 127.3, 126.2, 124.8, 124.2, 124.1, 122.8, 116.8, 116.7, 115.6, 115.0, 92.3, 89.5, 49.3, 31.6, 22.7, 20.1, 11.3, 11.2;

^{11}B NMR (160 MHz, $CDCl_3$) δ 0.92 (t, $J_{B\text{-}F}$ = 31.1 Hz). **^{19}F NMR** (471 MHz, $CDCl_3$) δ -130.42 (q, $J_{F\text{-}B}$ = 31.1 Hz). **HRMS** (ESI) *m/z*: $[M + Na]^+$ calcd for $C_{62}H_{44}BF_2N_5S_4Na$: 1058.2409; found 1058.2443.

Acknowledgments

This research was supported by the US-National Science Foundation (2000988 to FD), Science and Engineering Research Board (SERB) Project No. CRG/2022/000023 and STR/2022/000001, New Delhi. We gratefully acknowledge the Sophisticated Instrumentation Centre (SIC), IIT Indore. D. P. is thankful to CSIR, India for a research fellowship.

Conflict of Interests

The authors declare no conflict of interest

Data Availability Statement

The data that support the findings of this study are available in the supplementary material of this article.

Keywords: azaBODIPY, charge separation, electron transfer, nitrogenous donors, push-pull systems

References

[1] M. R. Wasielewski, *Acc. Chem. Res.* **2009**, *42*, 1910–1921.

[2] S. D. Straight, G. Kodis, Y. Terazono, M. Hambourger, T. A. Moore, A. L. Moore, D. Gust, *Nat. Nanotechnol.* **2008**, *3*, 280–283.

[3] G. Bottari, G. de la Torre, D. M. Guldi, T. Torres, *Chem. Rev.* **2010**, *110*, 6768–6816.

[4] D. M. Guldi, V. Sgobba, *Chem. Commun.* **2011**, *47*, 606–610.

[5] F. D'Souza, O. Ito, *Chem. Soc. Rev.* **2012**, *41*, 86–96.

[6] F. D'Souza, O. Ito, *Ed Kim Pan Stanf. Publ. Singap.* **2012**, *8*, 389–437.

[7] H. Imahori, T. Umeyama, S. Ito, *Acc. Chem. Res.* **2009**, *42*, 1809–1818.

[8] C. B. Kc, F. D'Souza, *Coord. Chem. Rev.* **2016**, *322*, 104–141.

[9] J. Zhang, W. Xu, P. Sheng, G. Zhao, D. Zhu, *Acc. Chem. Res.* **2017**, *50*, 1654–1662.

[10] M. Sommer, S. Huettner, M. Thelakkat, *J. Mater. Chem.* **2010**, *20*, 10788–10797.

[11] C. Deibel, T. Strobel, V. Dyakonov, *Adv. Mater.* **2010**, *22*, 4097–4111.

[12] V. Balzani, A. Credi, M. Venturi, *ChemSusChem* **2008**, *1*, 26–58.

[13] N. Armaroli, V. Balzani, *Angew. Chem. Int. Ed.* **2007**, *46*, 52–66.

[14] P. M. Beaujuge, J. M. J. Fréchet, *J. Am. Chem. Soc.* **2011**, *133*, 20009–20029.

[15] L. Hammarström, *Acc. Chem. Res.* **2015**, *48*, 840–850.

[16] T. Torres, G. Bottari, *Organic Nanomaterials: Synthesis, Characterization, and Device Applications*, John Wiley & Sons, **2013**.

[17] Y. Wu, W. Zhu, *Chem. Soc. Rev.* **2013**, *42*, 2039–2058.

[18] R. Misra, S. P. Bhattacharyya, *Intramolecular Charge Transfer: Theory and Applications*, John Wiley & Sons, **2018**.

[19] V. May, O. Kühn, *Charge and Energy Transfer Dynamics in Molecular Systems*, Wiley-VCH-Verlag, Weinheim, **2011**.

[20] S. Fukuzumi, K. Ohkubo, T. Suenobu, *Acc. Chem. Res.* **2014**, *47*, 1455–1464.

[21] M. Barrejón, L. M. Arellano, F. D'Souza, F. Langa, *Nanoscale* **2019**, *11*, 14978–14992.

[22] J. Yang, D. Kim, *Philos. Trans. R. Soc. Math. Phys. Eng. Sci.* **2012**, *370*, 3802–3818.

[23] T. Higashino, T. Yamada, M. Yamamoto, A. Furube, N. V. Tkachenko, T. Miura, Y. Kobori, R. Jono, K. Yamashita, H. Imahori, *Angew. Chem.* **2016**, *128*, 639–643.

[24] N. Zarrabi, S. Seetharaman, S. Chaudhuri, N. Holzer, V. S. Batista, A. Van Der Est, F. D'Souza, P. K. Poddutoori, *J. Am. Chem. Soc.* **2020**, *142*, 10008–10024.

[25] R. Canton-Vitoria, H. B. Gobeze, V. M. Blas-Ferrando, J. Ortiz, Y. Jang, F. Fernández-Lázaro, Á. Sastre-Santos, Y. Nakanishi, H. Shinohara, F. D'Souza, *Angew. Chem.* **2019**, *131*, 5768–5773.

[26] S. I. van Dijk, C. P. Groen, F. Hartl, A. M. Brouwer, J. W. Verhoeven, *J. Am. Chem. Soc.* **1996**, *118*, 8425–8432.

[27] C. O. Obondi, G. N. Lim, B. Churchill, P. K. Poddutoori, A. van der Est, F. D'Souza, *Nanoscale* **2016**, *8*, 8333–8344.

[28] M. Kivala, C. Boudon, J.-P. Gisselbrecht, P. Seiler, M. Gross, F. Diederich, *Angew. Chem. Int. Ed.* **2007**, *46*, 6357–6360.

[29] Y. Ge, D. F. O'Shea, *Chem. Soc. Rev.* **2016**, *45*, 3846–3864.

[30] A. Loudet, K. Burgess, *Chem. Rev.* **2007**, *107*, 4891–4932.

[31] G. Ulrich, R. Ziessel, A. Harriman, *Angew. Chem. Int. Ed.* **2008**, *47*, 1184–1201.

[32] M. E. El-Khouly, S. Fukuzumi, F. D'Souza, *ChemPhysChem* **2014**, *15*, 30–47.

[33] Z. Shi, X. Han, W. Hu, H. Bai, B. Peng, L. Ji, Q. Fan, L. Li, W. Huang, *Chem. Soc. Rev.* **2020**, *49*, 7533–7567.

[34] P. Rana, N. Singh, P. Majumdar, S. Prakash Singh, *Coord. Chem. Rev.* **2022**, *470*, 214698.

[35] K. Chen, Y. Dong, X. Zhao, M. Imran, G. Tang, J. Zhao, Q. Liu, *Front. Chem.* **2019**, *7*.

[36] A. N. Amin, M. E. El-Khouly, N. K. Subbaiyan, M. E. Zandler, M. Supur, S. Fukuzumi, F. D'Souza, *J. Phys. Chem. A* **2011**, *115*, 9810–9819.

[37] A. N. Amin, M. E. El-Khouly, N. K. Subbaiyan, M. E. Zandler, S. Fukuzumi, F. D'Souza, *Chem. Commun.* **2011**, *48*, 206–208.

[38] M. E. El-Khouly, A. N. Amin, M. E. Zandler, S. Fukuzumi, F. D'Souza, *Chem. Eur. J.* **2012**, *18*, 5239–5247.

[39] F. D'Souza, A. N. Amin, M. E. El-Khouly, N. K. Subbaiyan, M. E. Zandler, S. Fukuzumi, *J. Am. Chem. Soc.* **2012**, *134*, 654–664.

[40] V. Bandi, K. Ohkubo, S. Fukuzumi, F. D'Souza, *Chem. Commun.* **2013**, *49*, 2867–2869.

[41] S. K. Meher, G. R. Rao, *J. Phys. Chem. C* **2013**, *117*, 4888–4900.

[42] M. A. Collini, M. B. Thomas, V. Bandi, P. A. Karr, F. D'Souza, *Chem. – Eur. J.* **2017**, *23*, 4450–4461.

[43] D. Pinjari, A. Z. Alsaleh, Y. Patil, R. Misra, F. D'Souza, *Angew. Chem. Int. Ed.* **2020**, *59*, 23697–23705.

[44] S. Guo, L. Ma, J. Zhao, B. Küçüköz, A. Karatay, M. Hayvali, H. Gul Yaglioglu, A. Elmali, *Chem. Sci.* **2014**, *5*, 489–500.

[45] S. Kumar, K. G. Thorat, M. Ravikanth, *J. Org. Chem.* **2017**, *82*, 6568–6577.

[46] A. Koch, M. Ravikanth, *J. Org. Chem.* **2019**, *84*, 10775–10784.

[47] Q. Bellier, S. Pégaz, C. Aronica, B. L. Guennic, C. Andraud, O. Maury, *Org. Lett.* **2011**, *13*, 22–25.

[48] N. Balsukuri, S. Mori, I. Gupta, *J. Porphyr. Phthalocyanines* **2016**, *20*, 719–729.

[49] A. Koch, M. Ravikanth, *Eur. J. Org. Chem.* **2018**, *2018*, 228–234.

[50] N. Balsukuri, N. Jyoti Boruah, P. E. Kesavan, I. Gupta, *New J. Chem.* **2018**, *42*, 5875–5888.

[51] N. Balsukuri, M. Y. Lone, P. C. Jha, S. Mori, I. Gupta, *Chem. - Asian J.* **2016**, *11*, 1572–1587.

[52] Y. Gawale, N. Adarsh, S. K. Kalva, J. Joseph, M. Pramanik, D. Ramaiah, N. Sekar, *Chem. - Eur. J.* **2017**, *23*, 6570–6578.

[53] Ł. Łapok, I. Cieślar, T. Pędziński, K. M. Stadnicka, M. Nowakowska, *ChemPhysChem* **2020**, *21*, 725–740.

[54] B. Anjaiah, M. Naga Rajesh, L. Giribabu, R. Chitta, *Chem. – Asian J.* **2023**, e202300050.

[55] G. Rotas, M. B. Thomas, R. Canton-Vitoria, F. D'Souza, N. Tagmatarchis, *Chem. – Eur. J.* **2020**, *26*, 6652–6661.

[56] N. Balsukuri, N. Manav, M. Y. Lone, S. Mori, A. Das, P. Sen, I. Gupta, *Dyes Pigments* **2020**, *176*, 108249.

[57] *Gaussian 16*, Revision C.A03, M. J. Frisch, G. W. Trucks, H. B. Schlegel, G. E. Scuseria, M. A. Robb, J. R. Cheeseman, G. Scalmani, V. Barone, B. Mennucci, G. A. Petersson, H. Nakatsuji, M. Caricato, X. Li, H. P. Hratchian, A. F. Izmaylov, J. Bloino, G. Zheng, J. L. Sonnenberg, M. Hada, M. Ehara, K. Toyota, R. Fukuda, J. Hasegawa, M. Ishida, T. Nakajima, Y. Honda, O. Kitao, H. Nakai, T. Vreven, J. A. , Jr. , Montgomery, J. E. Peralta, F. Ogliaro, M. Bearpark, J. J. Heyd, E. Brothers, K. N. Kudin, V. N. Staroverov, R. Kobayashi, J. Normand, K. Raghavachari, A. Rendell, J. C. Burant, S. S. Iyengar, J. Tomasi, M. Cossi, N. Rega, J. M. Millam, M. Klene, J. E. Knox, J. B. Cross, V. Bakken, C. Adamo, J. Jaramillo, R. Gomperts, R. E. Stratmann, O. Yazyev, A. J. Austin, R. Cammi, C. Pomelli, J. W. Ochterski, R. L. Martin, K. Morokuma, V. G. Zakrzewski, G. A. Voth, P. Salvador, J. J. Dannenberg, S. Dapprich, A. D. Daniels, Ö. Farkas, J. B. Foresman, J. V. Ortiz, J. Cioslowski, D. J. Fox, Gaussian, Inc., Wallingford, CT, USA, **2016.**

[58] D. Rehm, A. Weller, *Isr. J. Chem.* **1970**, *8*, 259–271.

[59] J. J. Snellenburg, S. Laptenok, R. Seger, K. M. Mullen, I. H. M. van Stokkum, *J. Stat. Softw.* **2012**, *49*, 1–22.

Entry for the Table of Contents

A new series of donor-acceptor constructs featuring azaBODIPY and nitrogenous donors have been newly designed, synthesized and characterized using a range of physico-chemical techniques. Excited state charge transfer and separation, as a function of solvent polarity, is demonstrated by using femtosecond transient absorption spectroscopy.

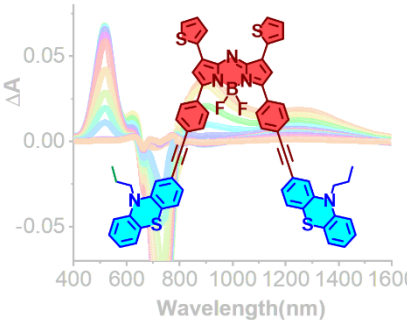

A. Z. Alsaleh D. Pinjari, R. Misra and F. D'Souza**

Page No. – Page No.

Far-Red Excitation Induced Electron Transfer in Bis Donor-AzaBODIPY Push-pull systems; Role of Nitrogenous Donors in Promoting Charge Separation

Twitter:
@iitindore
@UNTChemistry